Equivalent Model of Transient Gyrotron Cathode Response

Weiye Xu ⃝iD, *Member, IEEE*, Handong Xu, Fukun Liu, Xiaojie Wang, Yong Yang, and Jian Zhang

Abstract— The cathode power supply is one of the most important ancillary devices of gyrotrons. Some interesting transient phenomena about the cathode voltage and the cathode current were found in the gyrotron operation in the electron cyclotron (EC) resonance heating system of the Experimental Advanced Superconducting Tokamak. The cathode voltage drops to about 10% of the original value in about 90 μs in the overcurrent case, which is much longer than the 25 μs in the normal case. In order to explain these phenomena, an equivalent circuit model of the magnetron injection gun was proposed. The equivalent circuit is composed of parallel resistors and capacitors, and it can explain the test results very well. Using the equivalent circuit model to analyze gyrotrons can be an effective means of developing and operating an EC heating system.

Index Terms— Cathode, electron cyclotron (EC) heating, electron gun, equivalent circuit model, gyrotron, transient response.

I. INTRODUCTION

THE electron cyclotron (EC) system is an important plasma heating and current drive method. It is widely used for various fusion experimental devices [1]–[10], and it is also an important auxiliary heating system for ITER [11], [12].

A 140-GHz/4-MW EC resonance heating (ECRH) system consisting of four gyrotrons for the Experimental Advanced Superconducting Tokamak (EAST) is being developed in the Institute of Plasma Physics Chinese Academy of Sciences (ASIPP) [13]. Up to now, the first three gyrotrons have been tested and the fourth gyrotron is being manufactured in Communications & Power Industries LLC (CPI). The control and protection system, the data acquisition system [14], and the power measurement system [15] were built for the gyrotrons. In the commissioning process of the first three gyrotrons, many studies related to the gyrotron were done. In a recent experiment, #1 gyrotron oscillations of 980 kW/1 s and 650 kW/754 s, #2 gyrotron oscillations of 647 kW/2 s and 499 kW/80 s, and #3 gyrotron oscillations of 787 kW/20 s, 637 kW/100 s, and 559 kW/1000 s were demonstrated [16].
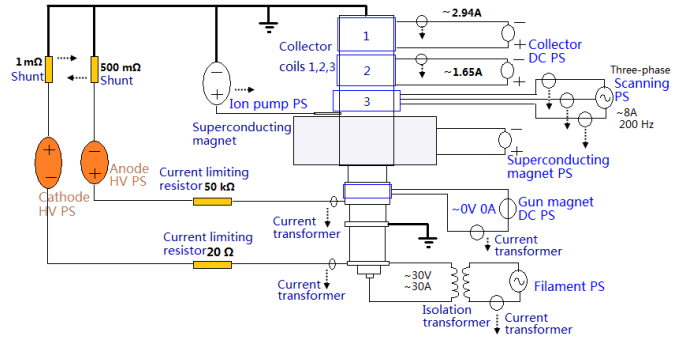
Fig. 1.   Gyrotron and its ancillary systems. "PS" in this figure is the short form for "power supply" and "HV" is for "high voltage."

The output power was measured using the calorimetric method [17], [18].

Currently, many studies about gyrotrons such as the beam–wave interaction theory [19], [20], the design of the gyrotron [21], transient effects of the output wave [22], and transient millimeter-wave signal analysis [23] are being done throughout the world. However, there is little research on the transient analysis of the cathode voltage, cathode current, anode voltage, anode current, and so on. Analysis of the transient behavior of the gyrotron cathode voltage and current can help us understand the internal state of the gyrotron. We have found some interesting phenomena in the operation of #1 gyrotron. An equivalent model of the magnetron injection gun was proposed to explain the test results in this article.

First, let us introduce the architecture and the schematic of the gyrotron and its ancillary systems and the timing sequence of the gyrotron. The gyrotron cannot work without its ancillary systems such as the superconducting magnet and its power supply, the collector power supply, the cathode power supply, the anode power supply, the ion pump power supply, and the filament power supply. The ancillary systems and their connections to the gyrotron are presented in Fig. 1. The current limiting resistors are used to limit the maximum current flowing through the cathode and the anode (50 kΩ for the anode and 20 Ω for the cathode). The dc shunts, which are actually resistors with a small resistance value, are used to measure the anode current and the beam current (500 mΩ for the anode current and 1 mΩ for the cathode current). Because the filament floats on the cathode high voltage, an isolation transformer is used between the filament and its power supply to protect the filament power source.
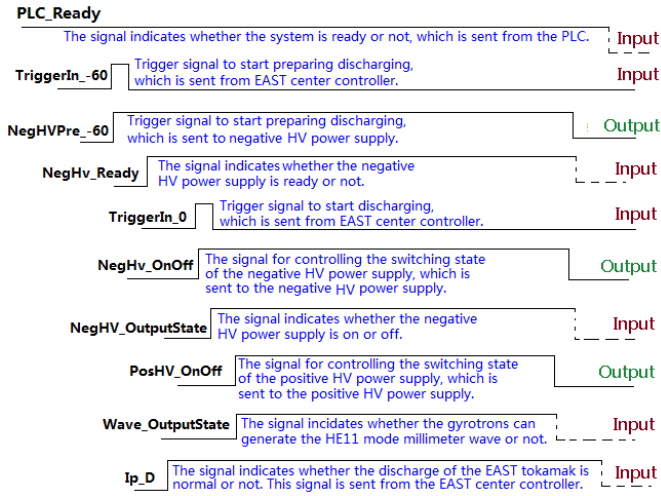
Fig. 2. Operation sequence of the gyrotron. The signals that are marked as "Input" indicate that the signals are input to the timing controller. The signals that are marked as "Output" indicate that the signals are output from the timing controller.

Fig. 3. Schematic of the cathode power supply whose nominal parameter is −60 kV/80 A/1000 s for gyrotrons. The power supply is composed of 87 PSM modules and 1 regulative pulse-step modulation (RPSM) module using the BUCK circuit.

The gyrotrons must be operated in a right timing sequence, otherwise the gyrotrons may be damaged. The right timing sequence is shown in Fig. 2. The PLC_Ready signal is an interlock signal from the programmable logic controller (PLC). The TriggerIn_-60 signal is sent from the EAST center controller; if the rising edge is detected by the timing controller, the timing controller will change the NegHVPre_-60 signal to a high level. In addition, the NegHVPre_-60 signal is sent to the cathode power supply; if the NegHVPre_-60 signal is at the high level, the switchgear of the cathode power supply will close. If the switchgear of the cathode power supply is closed, the cathode power supply will send a NegHv_Ready signal to the timing controller. 60 s after the rising edge of the TriggerIn_-60 signal is detected, a rising edge of the TriggerIn_0 signal will be sent to the timing controller. Then, the timing controller will turn the NegHv_OnOff signal to a high level immediately (in several nanoseconds). Then, the insulated gate bipolar transistors (IGBTs) of the cathode power supply will close according to the set time. If the output voltage of the cathode power supply is bigger than 30 kV, the NegHV_OutputState signal will be at the high level. 50 ms after the NegHv_OnOff signal changed to a high level, the timing controller will turn the PosHV_OnOff signal to a high level to turn on the anode power supply. 1 ms after the anode power supply is turned on, the timing controller will detect the Wave_OutputState signal (RF signal) to realize part of the RF protection [15]. If the Wave_OutputState signal becomes low, the shutdown procedure will start, i.e., the NegHv_OnOff signal and the PosHV_OnOff signal will be set to a low level successively (an interval of 2 ms), to shut down the power supplies to protect the gyrotron. In the process of gyrotron discharge, if the Ip_D signal (plasma current signal sent from the EAST center controller) becomes low, the shutdown procedure will start to protect the EAST tokamak from being damaged by the millimeter wave output from the gyrotrons. For safety, if any one of these signals such as PLC_Ready,
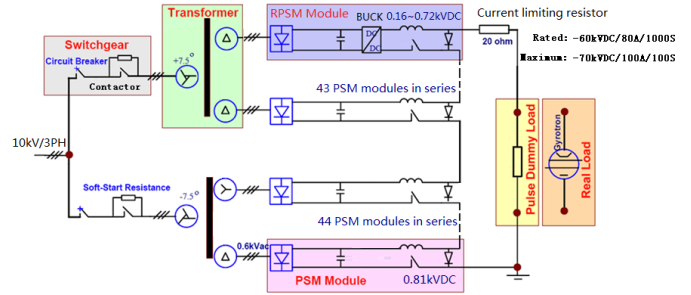
NegHv_Ready, NegHV_OutputState, Wave_OutputState, and Ip_D goes to a low level, the shutdown procedure will start.

The details of the transient analysis of the voltages and currents are discussed in the following sections. In Section II, the negative high-voltage power supply for gyrotrons is introduced. Then, in Section III, the measurement and analysis of the transient response of the cathode current and the cathode voltage are given. In Section IV, the equivalent circuit model of the gyrotron and its role in the analysis of gyrotron operation are discussed. Finally, we give a summary in Section V.

II. NEGATIVE HIGH-VOLTAGE POWER SUPPLY FOR GYROTRONS

We have developed two cathode high-voltage power supplies for four gyrotrons. The pulse-step modulation (PSM) technology was used in the cathode high-voltage power supply [24], which overcomes the shortcomings of the traditional high-voltage power supply, such as the large single volume, low efficiency, net side low harmonics pollution, lower power factor, larger output ripple, and slower dynamic response. The power supply topology is shown in Fig. 3. In order to protect the gyrotrons, it is necessary to ensure that the stored energy of the power supply system is small enough [25]. The energy is mainly stored in the output filter and stray capacitances for PSM modules. The stored energy is very small (<10 J) in our power supply system. In order to verify the protection effect, we have taken a short circuit test. A fuse (whose fusing energy is 10 J), which is connected in series in the loop, is still good when the load is shorted, which can prove that the stored output energy of the power supply is less than 10 J. Therefore, we can use this power supply for a gyrotron without the crowbar.

If the high-voltage source receives a turn-off signal or protection signal from the gyrotron control system, the IGBTs will shut down within several microseconds, thus the connection between the power supply and the gyrotron will be cut off. A test was made to verify the shutdown time of the cathode power source, which was found to be in several microseconds. A dummy load whose resistance value is 304 Ω was connected to the power source. The power supply shuts down when a turn-off signal is sent to the power supply. The waveforms of the voltage and the current of the cathode power supply when the IGBTs shut off are shown in Fig. 4. As we can see,
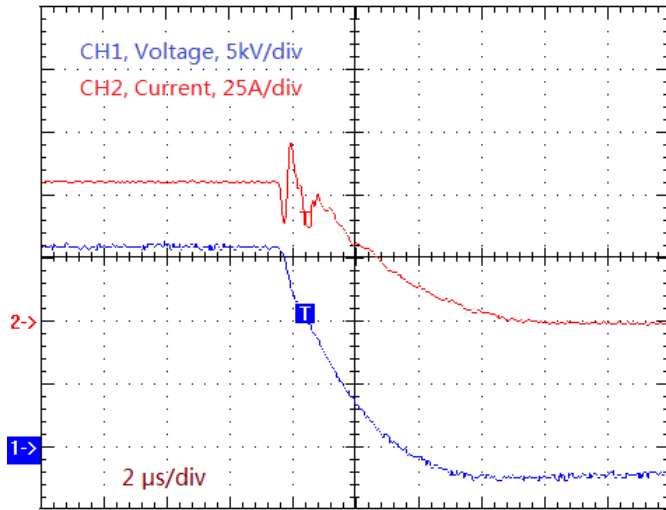
Fig. 4. Waveforms of the voltage and the current when the IGBTs shut off with a dummy load whose resistance value is 304 Ω.

Fig. 5. Measurement block diagram of the cathode voltage and the cathode current.

the shutdown time of the cathode power source is about 6 μs. It is short enough to protect the gyrotrons.

III. MEASUREMENT AND ANALYSIS OF THE TRANSIENT RESPONSE OF THE CATHODE CURRENT AND THE CATHODE VOLTAGE

The measurement block diagram of the cathode voltage and the cathode current is shown in Fig. 5. A high-voltage probe (max. frequency 20 MHz) that is in parallel with the cathode high-voltage power supply is used to measure the cathode voltage. A rapid response current probe (max. frequency 400 MHz) is used to measure the cathode current. The high-voltage probe and the current probe are both connected to the same oscilloscope, which is mainly used to measure the transient response. In addition, a shunt whose resistance is 1 mΩ is used to measure the cathode current. It is used to realize the slow overcurrent protection and to measure the steady-state cathode current.

Figs. 6 and 7 show the cathode voltage and the cathode current displayed on the oscilloscope when the gyrotron shuts down. As we can see, the response time of the cathode voltage when the gyrotron shuts down normally is different from the response time of the cathode voltage when the overcurrent protection happens. In the case of normal shutdown, the cathode voltage drops to about 10% of the original value for about 25 μs. In the case of overcurrent, the cathode voltage drops to about 10% of the original value for about 90 μs. Actually, in both cases, the circuit connection and the measurement method are identical, the only change factor is the gyrotron. The cathode voltage power supply always has the same shutdown process and the cathode power supply shuts down with the same operation within 6 μs. Therefore, we can infer that some gyrotron parameters change when an overcurrent happens. The change in the gyrotron parameter causes the change in the drop time of the cathode voltage. We proposed an equivalent model of the gyrotron gun to analyze it.
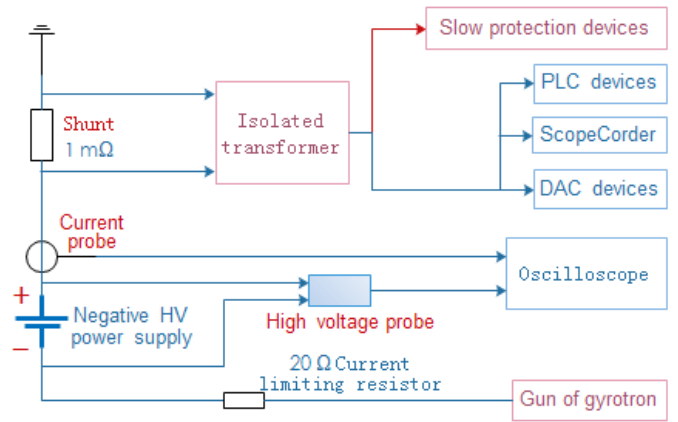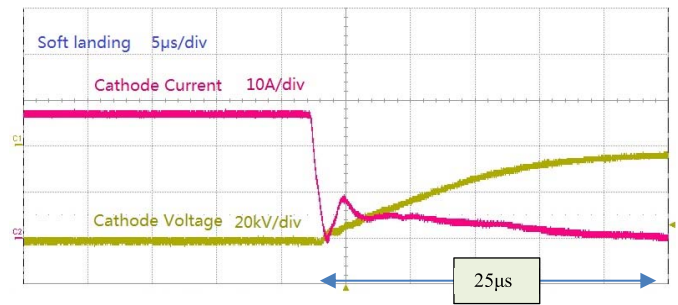

Fig. 6. Cathode voltage and the cathode current when the gyrotron shuts down normally.
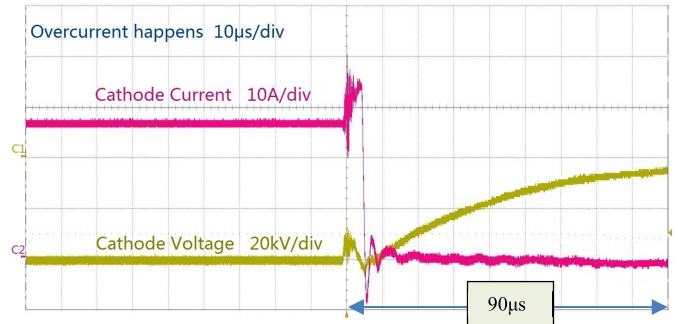

Fig. 7. Cathode voltage and the cathode current when the gyrotron shuts down with overcurrent.

The equivalent circuit of the gyrotron gun and the auxiliary power supplies are shown in Fig. 8, where R_{rb} is the cathode current limiting resistor with the resistance of 20 Ω; R_{ra} is the anode current limiting resistor with the resistance of 50 kΩ; R_{sb} is the shunt for measuring the beam current with the resistance of 1 mΩ; R_{sa} is the shunt for measuring the anode current with the resistance of 500 mΩ; R_b is the equivalent resistor of the electron gun between the cathode and the ground (body); C_b is the equivalent capacitor between the cathode and the ground (body); R_a is the equivalent resistor between the anode and the cathode; and C_a is the equivalent capacitor between the anode and the cathode.
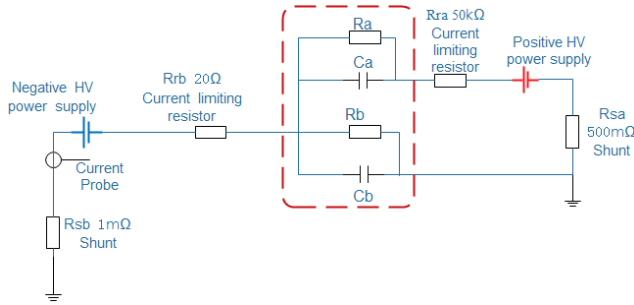
Fig. 8. Equivalent model of the gyrotron gun and the auxiliary power supplies. The equivalent model of the gun is in the red dashed box.

TABLE I

RESISTANCE OF Rb ALONG WITH THE CATHODE VOLTAGE, THE ANODE VOLTAGE, AND THE FILAMENT POWER

Cathode voltage [kV]	Anode voltage [kV]	Filament power [W]	Cathode Current [A]	R_b [kΩ]
-45	0	1135.32	32.2	1.3975
-44	0	1126.09	30.6	1.4379
-44	0	1113.26	30.1	1.4618
-43	0	1111.77	29.2	1.4726
-42	0	1099.59	26.5	1.5849
-42	0	1097.65	25.9	1.6216
-40	0	1097.65	25.6	1.5625
-35	0	1097.65	24.5	1.4286
-20	0	1097.65	20.0	1.0000
-10	0	1097.65	12.0	0.8333
-42	5	1099.59	27.3	1.5385
-42	16	1099.59	29.0	1.4483
-42	19	1099.59	29.4	1.4286

The resistance of R_b is related to the voltage across C_b and the voltage across C_a (the sum of the absolute value of the cathode voltage and the absolute value of the anode voltage) and the power of the filament power supply. In the case of the normal shutdown process of the cathode voltage, the anode voltage has been reduced to 0, so the value of R_b is only related to the voltage across C_b (cathode voltage) and the power of the filament power supply. Table I shows the examples.

We analyzed the relationship between the value of R_b and the cathode voltage u_b when the anode voltage is zero and the filament power is 1097.65 W. The relationship between the value of R_b and the absolute value of the cathode voltage u_b is shown in Fig. 9. We tried to fit the data in a variety of ways. The exponential fitting is more accurate, and the fitting function is given by

$$R_b = -359.6 + 1005.5 \times \exp(1.6 \times 10^{-5} u_b) \quad (1)$$

where the unit of u_b is volt and the unit of R_b is ohm.

When the cathode power supply shuts down, a capacitor discharge circuit is formed by C_b and R_b. That is,
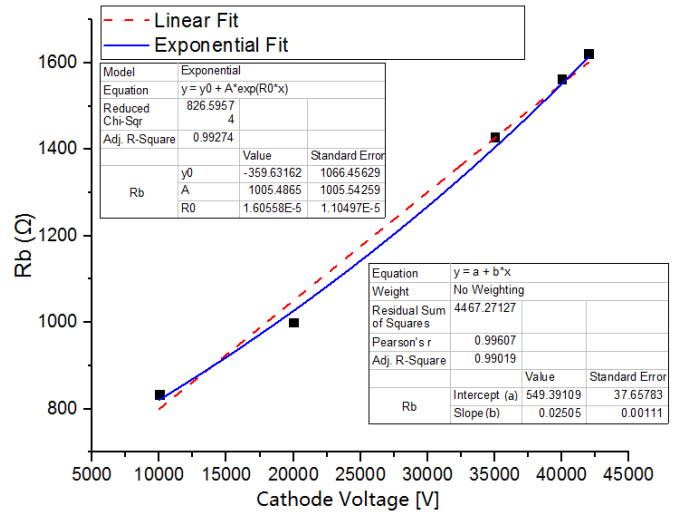

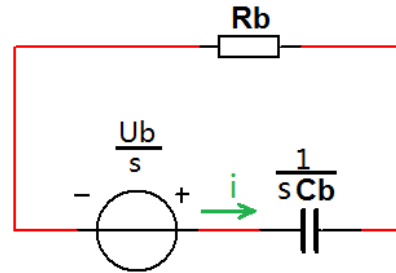Fig. 9. Value of R_b along with the cathode voltage.

Fig. 10. Laplace transform equivalent circuit when the cathode power supply shuts down.

a zero-input response. Assume the initial voltage across the capacitor C_b is U_b (a positive value in the unit of Volt), the Laplace transform equivalent circuit is shown in Fig. 10. The voltage across the capacitor C_b is

$$u(s) = \frac{U_b}{s} - \frac{\frac{U_b}{s} \cdot \frac{1}{sC_b}}{\frac{1}{sC_b} + R_b} = \frac{U_b}{s} - \frac{U_b}{s(1+sC_bR_b)} = \frac{U_b}{\frac{1}{C_bR_b} + s}. \quad (2)$$

Using the inverse Laplace transform, we can get

$$u(t) = U_b \times \exp\left(-\frac{1}{C_bR_b}t\right) \quad (3)$$

where $u(t) = u_b$. By solving (1) and (3), assume we can get (for convenience and without ambiguity, we will write $u(t) = u_b$ as u_t in the following):

$$u_t = U_b \times \exp\left(-\frac{1}{C_b(-359.6+1005.5 \cdot \exp(1.6 \times 10^{-5}u_t))}t\right). \quad (4)$$

Taking natural logarithm at both ends of (4) and simplifying the equation we get

$$359.6(\ln u_t - \ln U_b) + 1005.5(\ln U_b - \ln u_t)\exp(1.6 \times 10^{-5}u_t)$$
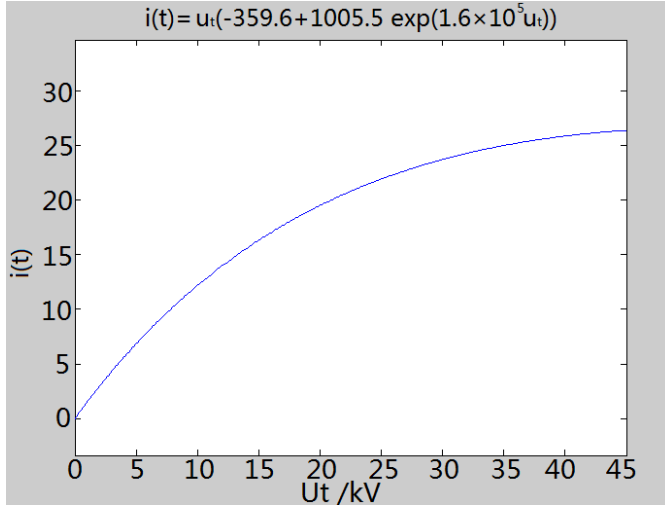$$= \frac{t}{C_b}. \quad (5)$$

Fig. 11. Current flowing through R_b as a function of voltage u_t.

Fig. 12. Equivalent model of the gyrotron gun and its power supplies with the crowbar switch.

Let $U_b = 41\,000$ V and $u_t = 4100$ V, then we can get the time used for the cathode voltage decreasing to about 10% of the original value

$$t \approx 1644.2 C_b. \tag{6}$$

As shown in Fig. 6, in the case of normal shutdown, the cathode voltage drops to about 10% of the original value for about 25 μs. So, the equivalent capacitance is

$$C_b \approx \frac{t}{1644.2} \approx 15.2 \text{ nF}. \tag{7}$$

For the current flowing through R_b, we assume the direction of the current as shown in Fig. 10 is positive, then

$$i(t) = -C_b \frac{du_t}{dt} = \frac{U_b}{R_b} \times \exp\left(-\frac{1}{C_b R_b}t\right). \tag{8}$$

Since R_b varies with the voltage u_t, (3) is substituted into (8) to obtain the relationship between the current $i(t)$ and the voltage u_t

$$i(t) = \frac{u_t}{R_b} = \frac{u_t}{-359.6 + 1005.5 \cdot \exp\left(1.6 \times 10^{-5} u_t\right)}. \tag{9}$$

The value of $i(t)$ is always positive, indicating that the actual direction of the current is the same as the direction shown in Fig. 10, i.e., the actual direction of the current is the same as the direction at time 0_-. The relationship between $i(t)$ and u_t is shown in Fig. 11. When $u_t = 41\,000$ V, $i(t) \approx 26$ A $= i(0\text{-})$; when $u_t = 30\,000$, $i(t) \approx 24$ A; when $u_t = 20\,000$ V, $i(t) \approx 20$ A; and when $u_t = 0$ V, $i(t) \approx 0$ A. The value of $i(t)$ decreases with the decrease of u_t, and the drop time is almost the same. It should be noted that the current $i(t)$ is the current flowing through the resistor R_b; it is not the same one measured by a current probe shown in Fig. 5, and it is hard to be measured.

The cathode current will increase suddenly (overcurrent happens) when a small discharge occurs or some other factors change inside the gyrotron gun. It is dangerous for the gyrotron. Therefore, if an overcurrent happens, the protection system will shut do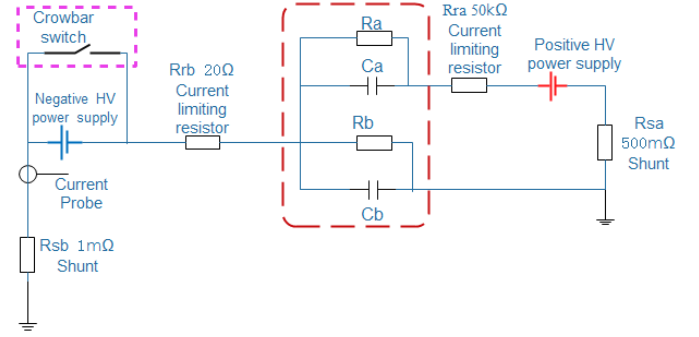wn the anode power supply and the cathode power supply at the same time. As we can see in Fig. 7, about 5 μs after overcurrent happens, the voltage began to turn off. Therefore, after overcurrent happens, the energy transmitted to the gyrotron is

$$W \approx \int p\,dt \approx \int_0^{5\mu} ui\,dt \approx 41 \text{ kV} \times 35 \text{ A} \times 5 \ \mu\text{s} \approx 7.2 \text{ J}. \tag{10}$$

In the situation where overcurrent happens, the anode voltage starts to decrease at the same time as the cathode voltage. That is, the anode voltage is not zero when the cathode power supply shuts down. But we can see from Table I that the value of R_b is less affected by the anode voltage. For the sake of simplicity, we ignore the anode voltage in the overcurrent situation. As we can see in Fig. 7, the cathode voltage drops to about 10% of the original value for about 90 μs, which is much longer than the time in the normal situation. The equivalent capacitance is

$$C_b \approx \frac{t}{1644.2} \approx 54.7 \text{ nF}. \tag{11}$$

The equivalent capacitance C_b increase may be due to the discharge between the cathode and the ground, which leads to the increase of the drop time of the cathode voltage.

In order to further verify the above assumptions, we try to add a crowbar short-circuit switch at both ends of the cathode voltage source. When the cathode voltage source is turned off, the crowbar short-circuit switch is automatically closed and the equivalent circuit is shown in Fig. 12. When the crowbar switch is closed, the capacitor C_b will be discharged through the R_{rb}. The voltage across the capacitor C_b is given by

$$u(t) = U_b \times \exp\left(-\frac{1}{C_b R_{rb}}t\right). \tag{12}$$

The cathode voltage drops to about 10% of the original value for about

$$2.3 R_{rb} C_b \approx 0.7 \ \mu\text{s}. \tag{13}$$

The actual cathode voltage waveform is shown in Fig. 13, and it can be seen that the voltage falling edge is indeed about 0.7 μs. However, because the voltage source turns off too fast, the oscillation of the voltage will be generated [26]. The oscillation occurs due to the signal transmission and reflection between the left end of the C_b and the ground.
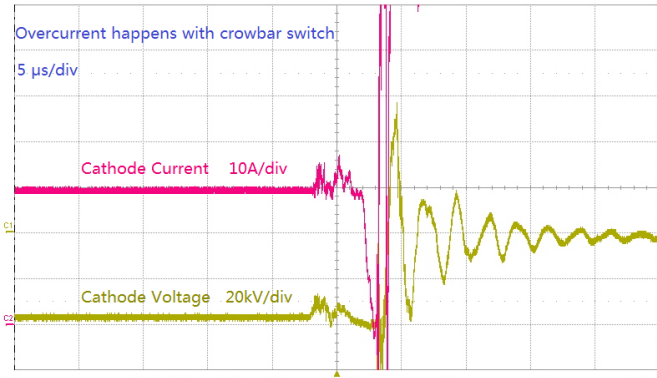
Fig. 13. Cathode voltage and the cathode current in the case the gyrotron shuts down when overcurrent happens with the crowbar switch.
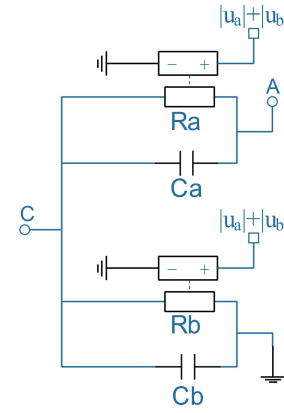

Fig. 14. Simplified equivalent circuit model of the gyrotron. "C" indicates the cathode power supply terminal and "A" indicates the anode power supply terminal. R_a and R_b are the voltage-controlled resistors.

The current flowing through R_{rb} is

$$i(t) = -C_b \frac{du_t}{dt} = \frac{U_b}{R_{rb}} \times \exp\left(-\frac{1}{C_b R_{rb}} t\right). \quad (14)$$

When $U_b = 41$ kV, the current is about 2.05 kA at time zero, and the current direction flowing through R_{rb} is opposite to the initial direction. Then, it decreases to about 205 A after 0.7 μs and to about 20.5 A after 1.4 μs. It can be seen from the beam current signal in Fig. 13 that the current signal rushes to a large value, but since the oscilloscope's preset signal amplitude range is small, we do not see how much the specific maximum value is. It can be seen from Fig. 13 that the current signal drops to near 0 A for about 1 μs, which is in line with the theoretical expectation. However, owing to the fact that the current edge is too fast, the current signal is transmitted back and forth on the signal line, and the current oscillation occurs.

The transient response of the anode current and the anode voltage when the power supply shuts down is similar to that of the cathode. The equivalent resistor R_a shown in Fig. 8 is related to the voltage across C_a (the sum of the absolute value of the cathode voltage and the absolute value of the anode voltage). The resistance of R_a decreases as the anode voltage increases. R_a is probably of several megohms; C_a is probably of several picofarads, and C_a may increase in the overcurrent condition. The time of the anode voltage drop to about 10% of the original value in the overcurrent case may be longer than that in the normal case. If just the cathode voltage is applied to the gyrotron, and the anode is not connected to the anode power supply or ground, the potential on the anode will be equal to the potential on the cathode. If the anode potential is not equal to the cathode potential, there may be an equivalent resistor between the anode and the ground. More detailed analysis and test will be made in the future.

IV. EQUIVALENT CIRCUIT MODEL OF THE GYROTRON AND ITS ROLE IN ANALYSIS OF GYROTRON OPERATION

We proposed an equivalent circuit model of the gyrotron gun in Section III. Actually, the gyrotrons can be analyzed using the same equivalent circuit model, which is shown in Fig. 14, where R_b is the equivalent resistor of the gyrotron between the cathode and the ground; C_b is the equivalent capacitor

between the cathode and the ground; R_a is the equivalent resistor between the anode and the cathode; and C_a is the equivalent capacitor between the anode and the cathode.

In the normal discharge of the gyrotron, the value of R_b is related to the filament power, the cathode voltage, the anode voltage, the pulse duration, etc. The value of R_b decreases as the filament power becomes higher, the anode voltage becomes higher, or the cathode voltage (absolute value) becomes higher. Usually, the beam current gradually decreases as the pulse time becomes longer [27], that is, the value of R_b increases as the pulse time becomes longer. The value of R_a is related to the anode voltage, the cathode voltage, and the magnetic field strength in the cathode region. When the magnetic field strength in the cathode region decreases, the anode current increases, resulting in a decrease in R_a. The values of C_a and C_b are closely connected with the electron beam generated by the magnetron injection gun. The different behavior of the gyrotron, especially during the fast turn-off of the high voltage triggered by an interlock, shows the dependency of the gyrotron characteristics on these capacitors.

The characteristics of the anode voltage, anode current, cathode voltage, and cathode current when the cathode power supply or the anode power supply is turned off can be analyzed using the method shown in Section III.

The beam current i_b can be calculated as

$$i_b = \frac{u_b}{R_b} \quad (15)$$

where u_b is the cathode voltage.

The anode current i_a can be calculated as

$$i_a = \frac{u_a + |u_b|}{R_a} \quad (16)$$

where u_a is the anode voltage.

The gyrotron output RF power P_{rf} can be calculated as

$$P_{rf} = \frac{u_b^2}{R_b} \eta \quad (17)$$

where η is the gyrotron efficiency, and it is related to the cathode voltage, the anode voltage, the magnetic field,

the filament power, and so on [28]. The gyrotron efficiency can also be measured.

In future, all the parameters of the equivalent circuit model of the gyrotron may be measured and provided by the gyrotron manufacturer. Therefore, gyrotron users like the Institutes for Fusion Research can use the gyrotrons more conveniently. It is useful for fusion heating research.

V. CONCLUSION

The gyrotron is a sophisticated vacuum device and many ancillary systems (such as the cathode power supply and the anode power supply) are needed to assist it in working. Gyrotrons must be operated at a right timing sequence to prevent them from being damaged. During the experiments of the #1 gyrotron, we found that the waveforms of the cathode voltage and the cathode current vary under different conditions. The cathode voltage drops to about 10% of the original value by about 90 μs in the overcurrent case, which is much longer than the 25 μs in the normal case. An equivalent circuit of the gun of the gyrotron is proposed to analyze the transient phenomena about the cathode voltage and the cathode current. The equivalent circuit is composed of parallel resistors and capacitors, and it can explain the test results well. We also simply predict the response of the anode voltage and the current according to the equivalent circuit model. The cathode transient response of #2 and #3 gyrotrons has not been tested since there was no idle time during the EAST experiment. More detailed tests will be made in the future. The proposed equivalent circuit model of the gyrotron in this article is meaningful. We can analyze the gyrotron like a chip using the equivalent circuit model. This may become an effective means of developing and operating an EC system in the future.

APPENDIX
COMPUTATION OF THE ZERO-INPUT RESPONSE

The Laplace transform equivalent circuit for zero-input response when the cathode power supply shuts down is shown in Fig. 10. Where the voltage source is not a real power source, it is the equivalent power source for the initial voltage across the capacitor C_b. During the discharge of the capacitor, the voltage across the capacitor C_b is actually equal to the voltage across the resistor R_b, which is

$$u(s) = \frac{U_b}{s} - \frac{\frac{U_b}{s} \cdot \frac{1}{sC_b}}{\frac{1}{sC_b} + R_b} = \frac{R_b \cdot \frac{U_b}{s}}{\frac{1}{sC_b} + R_b} = \frac{U_b}{\frac{1}{C_b R_b} + s}. \quad (18)$$

We can get the true voltage across the capacitor C_b as a function of time, as shown in (3), and the inverse Laplace transform of commonly used functions and the properties of the Laplace inverse transform are shown in the following equations:

$$\mathcal{L}^{-1}\left[\frac{1}{s-a}\right] = \exp(at) \quad (19)$$

$$\mathcal{L}^{-1}[bF(s)] = bf(t) \quad (20)$$

where a and b are constants.

REFERENCES

[1] V. Erckmann *et al.*, "ECRH and W7-X: An intriguing pair," in *Proc. AIP Conf. Proc.*, 2014, vol. 1580, no. 1, pp. 542–545.

[2] M. Lennholm *et al.*, "ECRH for JET: A feasibility study," *Fusion Eng. Des.*, vol. 86, nos. 6–8, pp. 805–809, Oct. 2011.

[3] J. Stober *et al.*, "ECRH on ASDEX upgrade—System status, feed-back control, plasma physics results," in *Proc. 17th Joint Workshop Electron Cyclotron Emission Electron Cyclotron Reson. Heating (EC)*, vol. 32, Sep. 2012, Art. no. 02011.

[4] A. V. Melnikov *et al.*, "Electric potential dynamics in OH and ECRH plasmas in the T-10 tokamak," *Nucl. Fusion*, vol. 53, no. 9, Sep. 2013, Art. no. 093019.

[5] X. T. Ding *et al.*, "Energetic particle physics experiments with high power ECRH on HL-2A," in *Proc. 17th Joint Workshop Electron Cyclotron Emission Electron Cyclotron Reson. Heating (EC)*, vol. 32, Sep. 2012, Art. no. 02002.

[6] G. P. Canal *et al.*, "Fast seeding of NTMs by sawtooth crashes in TCV and their preemption using ECRH," *Nucl. Fusion*, vol. 53, no. 11, Nov. 2013, Art. no. 113026.

[7] K. Hada *et al.*, "One-dimensional analysis of ECRH-assisted plasma start-up in JT-60SA," *Fusion Sci. Technol.*, vol. 67, no. 4, pp. 693–704, May 2015.

[8] H. Igami *et al.*, "Recent upgrading of ECRH system and studies to improve ECRH performance in the LHD," in *Proc. 18th Joint Workshop Electron Cyclotron Emission Electron Cyclotron Reson. Heating (EC)*, 2015, Art. no. 02011.

[9] M. Cengher *et al.*, "Advances in technology and high power performance of the ECH system on DIII-D," *Fusion Eng. Des.*, vol. 123, pp. 295–298, Nov. 2017.

[10] Y. S. Bae, J. Decker, J. H. Jeong, and K. D. Lee, "Study of synergetic effect of X2 and X3 EC wave in KSTAR," in *Proc. EPJ Web Conf.*, 2015, Art. no. 02015.

[11] M. Henderson *et al.*, "The targeted heating and current drive applications for the ITER electron cyclotron system," *Phys. Plasmas*, vol. 22, no. 2, 2015, Art. no. 021808.

[12] T. Omori *et al.*, "Progress in the ITER electron cyclotron heating and current drive system design," *Fusion Eng. Des.*, vols. 96–97, pp. 547–552, Oct. 2015.

[13] H. Xu *et al.*, "Development and preliminary commissioning results of a long pulse 140 GHz ECRH system on EAST tokamak (Invited)," *Plasma Sci. Technol.*, vol. 18, no. 4, pp. 442–448, 2016.

[14] W. Xu, H. Xu, F. Liu, F. Hou, and Z. Wu, "Data acquisition system for electron cyclotron resonance heating on EAST tokamak," *Fusion Eng. Des.*, vol. 113, pp. 119–125, Dec. 2016.

[15] W. Xu *et al.*, "Millimeter wave power monitoring in EAST ECRH system," *IEEE Access*, vol. 4, no. 1, pp. 5809–5817, 2016.

[16] W. Xu, H. Xu, F. Liu, H. Hu, and J. Feng, "Electromagnetic compatibility in electron cyclotron resonance heating system," *IEEE Trans. Plasma Sci.*, vol. 47, no. 5, pp. 1887–1894, May 2019.

[17] L. A. Gorelov *et al.*, "Gyrotron power balance based on calorimetric measurements in the DIII-D ECH system," in *Proc. 20th IEEE/NPSS Symp. Fusion Eng.*, Oct. 2003, pp. 546–548.

[18] W. Xu, H. Xu, F. Liu, J. Wang, X. Wang, and Y. Hou, "Calorimetric power measurements in the EAST ECRH system," *Plasma Sci. Technol.*, vol. 19, no. 10, 2017, Art. no. 105602.

[19] L. Shenggang, "The kinetic theory of electron cyclotron resonance maser," *Scientia Sinica*, vol. 22, no. 8, pp. 901–911, 1979.

[20] E. Borie and B. Jodicke, "Comments on the linear theory of the gyrotron," *IEEE Trans. Plasma Sci.*, vol. PS-16, no. 2, pp. 116–121, Apr. 1988.

[21] M. V. Kartikeyan, E. Borie, O. Drumm, S. Illy, B. Piosczyk, and M. Thumm, "Design of a 42-GHz 200-kW gyrotron operating at the second harmonic," *IEEE Trans. Microw. Theory Techn.*, vol. 52, no. 2, pp. 686–692, Feb. 2004.

[22] A. T. Lin, "Transient effects in high current gyrotrons," *Proc. SPIE*, vol. 0873, pp. 8–17, May 1988.

[23] A. Schlaich, G. Gantenbein, J. Jelonnek, and M. Thumm, "Transient millimeter-wave signal analysis with unambiguous RF spectrum reconstruction," *IEEE Trans. Microw. Theory Techn.*, vol. 61, no. 12, pp. 4660–4666, Dec. 2013.

[24] Z. Yang, J. Zhang, Y. Huang, X. Hao, Q. Zhao, and F. Guo, "The Analysis and Design of High Voltage DC power supply of ECRH for EAST," *Nucl. Sci. Technol.*, vol. 01, no. 1, pp. 9–17, 2013.

[25] P. Brand and G. A. Mueller, "Circuit design and simulation of a HV-supply controlling the power of 140 GHz 1 MW gyrotrons for ECRH on W7-X," *Fusion Eng. Des.*, vols. 66–68, pp. 573–577, Sep. 2003.

[26] H. W. Johnson and M. Graham, *High-Speed Digital Design: A Handbook of Black Magic*. Englewood Cliffs, NJ, USA: Prentice-Hall, 1993.

[27] T. E. Harris, "Active heater control and regulation for the Varian VGT-80 11 gyrotron," in *Proc. 14th IEEE/NPSS Symp. Fusion Eng.*, vol. 1, Sep./Oct. 1991, pp. 130–131.

[28] G. S. Nusinovich, M. K. A. Thumm, and M. I. Petelin, "The gyrotron at 50: Historical overview," *J. Infr. Millim. THz. Waves*, vol. 35, no. 4, pp. 325–381, Apr. 2014.
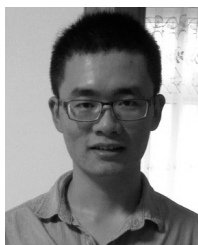
Weiye Xu (M'17) was born in Qufu, China, in 1990. He received the B.S. degree in electronic science and technology from Shandong Normal University, Jinan, China, in 2011, the Ph.D. degree in nuclear energy science and engineering from the University of Chinese Academy of Sciences, Beijing, China, in 2017.

He is currently an Assistant Professor with the Institute of Plasma Physics, Chinese Academy of Sciences, Hefei, China. His current research interests include the high-power microwave heating technology for plasma, electronic technology, electromagnetic field theory, and microwave technology.

Handong Xu was born in Yuexi County, China. He received the M.S. degree in microwave engineering from the Institute of Plasma Physics, Chinese Academy of Sciences, Hefei, China, in 2004, and the Ph.D. degree in advanced energy engineering from Kyushu University, Fukuoka, Japan, in 2008.

He participated in the research of 4-MW 2.45-GHz and 6-MW 4.6-GHz lower hybrid current drive (LHCD) on EAST from 2009 to 2011. He mainly studies 140-GHz 4-MW electron cyclotron resonance heating (ECRH) system and ECRH experiments on EAST from 2012. He is currently a Professor with the Institute of Plasma Physics, Chinese Academy of Sciences. His current research interests the development of high-power microwave heating and current drive system and corresponding experiment study on EAST Tokamak devices.

Fukun Liu is currently a Professor with the Institute of Plasma Physics, Chinese Academy of Sciences, Hefei, China. His current research interests include microwave technology and experimental plasma physics.

Xiaojie Wang is with the Institute of Plasma Physics, Chinese Academy of Sciences, Hefei, China. Her current research interests include microwave technology and experimental plasma physics.

Yong Yang is with the Institute of Plasma Physics, Chinese Academy of Sciences, Hefei, China. His current research interest includes electronic technology.

Jian Zhang is with the Institute of Plasma Physics, Chinese Academy of Sciences, Hefei, China. His current research interest includes the high-voltage power supply technology.